

Infection dynamics of a *V. splendidus* strain pathogenic to *Mytilus edulis* : *In vivo* and *in vitro* interactions with hemocytes

Ben Cheikh Yosra ^{1,*}, Travers Marie-Agnes ², Le Foll Frank ¹

¹ Univ Le Havre Normandie, FR CNRS Scale 3730, Environm Stresses & Aquat Biomonitoring, UMR I INERIS URCA ULH SEBIO 02, F-76063 Le Havre, France.

² IFREMER, SG2M, LGPMM, Ave Mus de Loup, F-17390 La Tremblade, France.

* Corresponding author : Yosra Ben Cheikh, email address : yosra_bencheikh@yahoo.fr

Abstract :

The pathogenic strain *V. splendidus* 10/068 1T1 has previously been reported for its virulence to the blue mussel and for its capacity to alter immune responses. In this study, we expanded the knowledge on hemocyte-pathogen interactions by using *in vitro* and *in vivo* assays. *V. splendidus* 10/068 1T1 severely inhibited cell adhesion and acidic vacuole formation unlike the innocuous phylogenetically related *V. splendidus* 12/056 M24T1 which had no effect on these cell functions. Furthermore, the virulent bacteria decreased hemocyte viability (59% of viability after 24 h). Infection dynamics were explored by using a model based on water tank cohabitation with septic mussels infected by GFP-tagged *V. splendidus* 10/068 1T1. Experimental infections were successfully produced (16.6% and 45% mortalities in 3 days and 6 days). The amount of GFP *Vibrio* in seawater decreased during the experiment suggesting its horizontal transfer from diseased animals to healthy ones. At the same time periods, bacteria were detected in hemocytes and in various organs and caused necrosis especially in gills. Total hemocyte count and viability were affected. Taken together, our results indicate that the pathogen *V. splendidus* 10/068 1T1 colonizes its host both by bypassing external defense barriers and impairing hemocyte defense activities.

Highlights

► Establishment of mussel experimental infection by *V. splendidus* via cohabitation. ► Detection of the GFP-*V. splendidus* strain in mussel tissues and hemocytes. ► Necrosis of gills during experimental infection by the virulent *Vibrio* strain. ► The virulent strain alter phagolysosome maturation, hemocyte adhesion and viability.

Keywords : Innate immunity, Bivalves, *Vibrio*, Infection, Experimental model, Hemocyte

56 **1. Introduction**

57 Heterotrophic bacteria belonging to the genus *Vibrio* are highly abundant in the aquatic
58 environment, mostly in seawater [1]. These ubiquitous microorganisms persist in a variety of
59 geographic areas in interaction with eukaryotic marine hosts including zooplankton, sponges,
60 corals and molluscs [1]. *Vibrio* sp. show a remarkable biodiversity. Until now, more than 110
61 species of *Vibrios* have been identified, displaying a variety of host association modalities that
62 extend from symbiosis to virulent pathogenicity [2,3].

63 Many species of pathogenic *Vibrios* are known to be responsible for diseases in terrestrial or
64 marine vertebrates and invertebrates. *Vibrio cholerae*, *Vibrio vulnificus* and *Vibrio*
65 *parahaemolyticus* in particular cause severe disorders in humans [4,5]. In numerous aquatic
66 organisms including fish [6], corals [7], shrimp [8] and shellfish [9], some *Vibrios* have been
67 associated with serious infections. Because of the high economic loss generated in the
68 aquaculture sector, many studies are dedicated to bacterial diseases, particularly in farmed
69 bivalves [3,9,10]. Among the etiological agents, bacteria from the clade *Splendidus* have been
70 repeatedly described in relation to mortality events. This polyphyletic group include 16 species
71 with contrasted pathotypes [11,12]. Different strains have been implicated in mortalities of
72 various bivalves, e.g. the Pacific oyster *Crassostrea gigas* [13–17], the Atlantic scallop *Pecten*
73 *maximus* [18,19], the carpet shell clam *Ruditapes philippinarum* [20], the greenshell mussel
74 *Perna canaliculus* [21] and recently the blue mussel *Mytilus edulis* [11].

75 While infection mechanisms are well studied in human invaders, little is known in the specific
76 case of invertebrate pathogens. Some results have been gathered in different species, especially
77 concerning host-pathogen interactions [11, 22–24]. However, invasion processes remain poorly
78 documented. Understanding infection dynamics is an essential step for developing diseases
79 management strategies [25]. In particular, there is a need for robust and standardized
80 experimental models of *Vibrio*-bivalve interactions.

81 In a previous work, from mortality events reported by mussel farmers, we have isolated a *Vibrio*
82 strain virulent to the blue mussel. *V. splendidus* 10/068 1T1 has been shown to alter hemocyte
83 phagocytosis capacities, a key parameter of the immune defense system in mussels.
84 Furthermore, a stable GFP-tagged *Vibrio* strain was constructed to facilitate the study of
85 interactions between the microorganism and immune cells [11]. Fluorescent proteins (FP)-
86 tagged microorganisms constitute a useful tool to monitor colonization processes. They have
87 been used to elucidate early invasion events in squids [26,27] and bacterial dynamics in filter
88 feeding oysters [28].

89 In the present study, we have investigated infection dynamics of *V. splendidus* 10/068 1T1 in
90 *Mytilus edulis*. We describe (i) the development of an experimental infection model by water
91 tank cohabitation with septic mussels, (ii) the localization of GFP bacteria in infected animals
92 with the corresponding tissue lesions and (iii) *in vitro/in vivo* interactions between the
93 pathogenic *Vibrio* strain and *Mytilus edulis* hemocytes.

94 **2. Material and methods**

95 **2.1. Mussel collection**

96 Adult mussels, *M. edulis* with shell length ranging from 4 to 5 cm, were collected on the
97 intertidal rocky shore of Yport (0°18'52"E:49°44'30"N, France) between December 2015 and
98 March 2016, immediately transported to the laboratory and placed in a temperature-controlled
99 (10°C) aerated Biotop Nano Cube 60 seawater tank (Sera, Heinsberg, Germany) , equipped
100 with mechanical and activated biological filtering. The animals were fed with algae (*Isochrysis*
101 *galbana*) and maintained in these conditions for at least one week before use.

102 **2.2. Bacterial strains and culture conditions**

103 Two parental and GFP-tagged *V. splendidus*-related strains were used in this study: a virulent
104 *V. splendidus* 10/068 1T1 isolated from mussel mortality events reported by professional
105 (French national surveillance network REPAMO) in 2010 and an innocuous *V. splendidus*
106 12/056 M24T1 isolated from mussel microflora in absence of mortality in the context of
107 Bivalife European project in 2012 [11]. Bacteria were routinely cultivated overnight in LBS
108 [Luria Bertani complemented with salt, NaCl 20 g.L⁻¹ (f.c.)] at 22°C. Stock cultures were stored
109 at -80°C in LBS with glycerol 15% (v/v) supplemented with kanamycin 100 µg.L⁻¹ for GFP-
110 tagged strains.

111 **2.3. In vitro hemocyte challenge**

112 **2.3.1. Hemolymph collection**

113 Hemolymph was withdrawn from the posterior adductor muscle sinus, by gentle aspiration with
114 a 1 mL syringe equipped with a 22G needle. Quality of samples was systematically checked by
115 microscopic observation before using in bioassays. Samples containing protozoa, tissue
116 fragments, low number of hemocytes were discarded.

117 **2.3.2. Hemocyte adhesion**

118 Cells were incubated with bacteria at a ratio of 10 bacteria/hemocyte, or with sterile
119 physiological water (NaCl 9 g.L⁻¹), in a 24-well tissue-culture plates (Greiner). After 2, 4 and

120 6 hours at 15°C, the number of non adherent cells in the supernatant was counted by flow
121 cytometer.

122 **2.3.3. Acidic vacuole formation**

123 Crude hemolymph was placed into individual wells of 24-well tissue-culture plates (Greiner)
124 for cytometry or in 35 mm μ -Dish (Ibidi) for microscopy. Cells were exposed to *Vibrio* strains
125 at 10:1 ratio (bacteria:hemocytes) for 2 hours at 15°C.

126 LysoTracker (LysoTracker® Green DND-26, life technologies) at 2 μ M was added and cells
127 were incubated for 30 minutes at 15°C in the dark. Hemocyte fluorescence was quantified by
128 flow cytometry. For microscopy imaging, cells were washed with the marine physiological
129 saline solution [MPSS (470 mM NaCl, 10 mM KCl, 10 mM CaCl₂, 10 mM HEPES, 48,7 mM
130 MgSO₄), pH 7.8, 0.2 μ m filtered]. Hemocyte nuclei were counterstained with hoechst 33342 (5
131 μ M, 15 min) and imaged by epifluorescence microscopy.

132 **2.3.4. Hemocyte viability**

133 Hemocytes were exposed to bacteria (10/068 1T1 and 12/056 M24T1) at 10⁸ CFU.mL⁻¹ for
134 different time periods (2, 4, 6, 18 and 24h) at 15°C. At each time point, propidium iodide was
135 added (20 μ M) and cell viability was measured by flow cytometry.

136 **2.4. *In vivo* challenge**

137 **2.4.1. Mussel infection by water tank cohabitation model**

138 Bacteria were prepared at OD_{600nm} of 1 as described in Ben Cheikh et al. [11]. Animals were
139 anesthetized for 2–3 h at 16°C in a magnesium chloride solution (50 g.L⁻¹, 1/4: v/v
140 seawater/freshwater) under aeration. Subsequently, a volume of 100 μ L of bacterial suspension
141 (2.10⁸ CFU.mL⁻¹) or filtered sterile seawater (FSSW) for the negative control was injected into
142 the posterior adductor muscle. After injection, the animals were transferred to tanks (3 replicate
143 tanks, 10 mussels per tank) filled with 2L of UV-treated and filtered seawater supplemented
144 with 50 mL of phytoplankton (*Isochrysis galbana*). After 24 hours, moribund animals were
145 sacrificed by severing their adductor muscle and placed in cohabitation with a group of 10
146 apparently healthy mussels. For the negative control, mussels injected with FSSW (alive) were
147 sacrificed and used in the same conditions. After 72 hours of cohabitation, injected mussels
148 were removed. During the experiment, animals were maintained under static conditions at 16°C
149 with aeration. Mortality was monitored each day over a six days period. Animals were
150 considered to be dead when the valves did not close following stimulation. Newly dead mussels
151 were removed from the tanks.

152 **2.4.2. Bacteria counting in seawater**

153 Seawater was sampled from cohabitation tanks each day during the experiment period. 100 μ L
154 of samples serially diluted in sterile physiological water (NaCl 9 g.L⁻¹) was plated on LBS agar
155 supplemented with kanamycin 100 μ g.L⁻¹. After 48h at 22°C, colonies were counted. The
156 presence of GFP colonies was verified under a fluorescence stereo microscope (Leica
157 microsystems).

158 **2.4.3. Hemocyte cellular parameters analysis**

159 Hemolymph was sampled from exposed mussels and mixed with cold Alsever's solution (300
160 mM NaCl, 100 mM Glucose, 30 mM sodium Citrate, 26 mM citric acid, 10 mM EDTA, pH
161 5.4) for cytometry analysis.

162 Variation in hemocyte count and the percentage of cells containing GFP-tagged bacteria was
163 determined. Cell viability was investigated by adding propidium iodide (20 μ M).

164 **2.4.4. Histological and Immunohistochemical analyses**

165 During cohabitation infection, mussels were sampled at different time periods and removed
166 from their shell. Tissues were fixed in Davidson's solution (20% formaldehyde 36%, 30%
167 FSSW, 10% glycerol, 30% ethanol 95% and 10% acetic acid) for 48h, dehydrated in a graded
168 series of ethanol, and embedded in paraffin. Consecutive 3-5 μ m thick sections were adhered
169 to Superfrost [hematoxylin-eosin (HE) staining] or Superfrost Plus [immunohistochemistry
170 (IHC)] microscope slides.

171 For tissue examination, sections were stained by classical hematoxylin-eosin protocol. Presence
172 of listed pathogens (*Bonamia* sp., *Marteilia* sp., *Perkinsus* sp. and *Mikrocytos* sp.) was
173 examined as well as trematods, copepods, *Mytilicola*, ciliates and gregarines. For lesions, we
174 noticed the presence of necrosis, bacterial "foyer", hemocytes infiltration and granulomas into
175 the different tissues: gills, gonads, digestive glands, mantle, muscle, kidney and digestive tube.
176 The lesions in each organ were coded as follows: 0 (absence of lesion); 1 (low), 2 (moderate),
177 3 (high). "Low" corresponds to at least one observation in 20 fields of the slide, "moderate"
178 corresponds to at least 5 observations in 10 fields of the slide and "high" corresponds to at least
179 10 observations in 10 fields of the slide.

180 For IHC, a polyclonal antibody raised in rabbit against recombinant full length GFP protein
181 was used (Ab290, Abcam). The specificity of this antiserum has been previously tested and
182 optimized. Immuno-labellings were performed with a Benchmark automate (Ventana-Roche)
183 by Histalim (Montpellier). Sections were incubated for 32 min with primary antibody (1:5000)
184 and revealed with Ultraview Red Alkaline Phosphatase kit (Roche Diagnostics). Slides were

185 finally numerized with a Nanozoomer x20 (Hamamatsu). Labeling of bacterial-like cells was
186 coded following the same criteria used for lesion observations: 0 (absence of labelling); 1 (low),
187 2 (moderate), 3 (high).

188 **2.5. Statistical analyses**

189 Statistical analysis was performed by using SigmaPlot 12 (Systat Software Inc., Chicago, IL).
190 Replicates were averaged and the values were tested for normality (Shapiro-Wilk) and paired
191 comparisons were performed by Student's t-tests or by Mann-Whitney rank sum tests in case of
192 unequal variance. Statistical significance was accepted for * $p < 0.05$, ** $p < 0.01$ or *** $p <$
193 0.001 .

194 **3. Results**

195 **3.1. Hemocyte adhesion**

196 The effect of *V. splendidus*-related strains on hemocyte-substrate adhesion was evaluated *in*
197 *vitro* for different time of incubation (**Figure 1**). Hemocyte attachment to the culture dish was
198 significantly affected after 2h of exposure to the virulent *V. splendidus* 10/068 1T1. Moreover,
199 the number of detached hemocytes increased for 6h incubations. In contrast, when exposed to
200 the innocuous *Vibrio* strain 12/056 M24T1, non-adherent cells increased slightly after 2h
201 exposure and then decreased.

202 **3.2. Acidic vacuole formation**

203 The capacity of *M. edulis* hemocytes to generate phagolysosome proliferation after exposure to
204 virulent and non-virulent bacteria *in vitro* was investigated by flow cytometry and
205 epifluorescence microscopy (**Figure 2**). The lysotracker signal, indicative of acidic vacuole
206 formation, was significantly higher in hemocytes challenged with the strain 12/056 M24T1 than
207 in cells co-cultured with the strain 10/068 1T1 ($p < 0.001$, **Figure 2a**). Moreover, in the case of
208 exposure to 12/056 M24T1, numerous phagolysosomal compartments surrounding the nucleus
209 can be found (**Figure 2b**). Microscopic observation also confirmed the absence of large acidic
210 compartments in cells challenged with the virulent strain.

211 **3.3. Hemocyte viability**

212 Hemocyte viability was monitored after exposure to *V. splendidus*- related strains for different
213 time durations. Cell viability was stable during the first 6 hours for both strains with values
214 corresponding to 92% of viable cells (**Figure 3**). Then, hemocyte viability slightly decreased
215 until 24h post exposure to the innocuous strain 12/056 M24T1, but was never lower than 80 %.
216 In contrast, for the same time periods, the viability of cells incubated with the strain 10/068 1T1

217 was significantly affected, reaching a percentage of viable cells of only 59% after 24h exposure
218 to the virulent strain.

219 **3.4. *Vibrio* infection by cohabitation challenge**

220 Experimental infection of mussels with the pathogenic *V. splendidus* 10/068 1T1 was obtained
221 by water tank cohabitation assays. First mortalities appeared after 3 days (16.6%) and increased
222 progressively to reach almost 45% at the 6th day (**Figure 4**). No mortality was observed in
223 control tanks.

224 **3.5. Seawater bacteria count during infection**

225 Bacteria seawater density in cohabitation tanks was monitored during infection (**Figure 5**).
226 After 48h of cohabitation, the *Vibrio* density reached 3.10^6 CFU/mL, then decreased
227 progressively to 2.10^3 CFU/mL after 5 days.

228 **3.6. Hemocyte parameters analysis during the experimental infection**

229 Different hemocyte parameters were investigated during cohabitation assays with septic
230 mussels infected by the virulent strain 10/068 1T1 (**Figure 6**). In hemolymph sampled from the
231 adductor muscle, the total hemocyte count increased significantly 48h after the cohabitation
232 onset and then decreased until the end of the exposure to reach control values (**Figure 6a**).
233 Interestingly, GFP bacteria were detected in hemocytes. The percentage of cells containing
234 GFP-tagged *Vibrio* was also higher at the beginning of the exposure and then decreased
235 progressively (**Figure 6b**). Furthermore, hemocyte viability slightly decreased compared to the
236 control but remained almost stable during *Vibrio* infection (80% of viable cells at day 2 and
237 74% at day 5, **Figure 6c**).

238 **3.7. Tissue infection by bacteria**

239 GFP-*Vibrios* were detected mainly in gills of 8 out of 31 live animals and 9 out of 9 moribund
240 animals, either in the pallial cavity, forming aggregates, attached to apical cilia or between
241 ordinary gill filaments (**Figure 7A, C**). Some labeling were also noticed in esophagi or stomach
242 of 4 out of 28 live animals (**Figure 7D**). Main observed lesions correspond to necrosis of
243 epithelia (gills and digestive tissues, respectively 30 and 8 out of 40 animals) and hemocyte
244 infiltrations (17 out of 40 animals), as well as granulomas in the mantle (17 out of 40 animals)
245 (**Figure 7B, supplementary figure 1C-E, Table 1**). Moribund animals contained bacteria in
246 large amounts and presented general necrosis patterns even if some organs were obviously not
247 affected (muscle, gonad, kidney and mantle) (**Figure 7B, Table 1**).

248 Some trematodes *metacercaria* in 36 out of 40 animals, copepods in 3 out of 40 animals, ciliates in
249 28 out of 40 animals or gregarines in 7 out of 40 animals, were noticed (**supplementary figure**
250 **1, Table 1**). However, the most noticeable microorganism present on hematoxylin-eosin
251 stained slides corresponds to bacteria. Seventeen of the 40 analyzed individuals present
252 bacterial cells into gills (8 low amount, 6 moderate and 3 high). Bacteria were also noticed in
253 digestive tissues (10 individuals – 6 low and 4 moderate) and mantle (9 individuals – 3 low and
254 6 moderate) (**supplementary figure 1D, Table 1**). No listed parasites were found in the 40
255 mussels (19 females and 21 males).

256 **4. Discussion**

257 In a previous study, we have reported the virulence of *V. splendidus* 10/068 1T1 to the blue
258 mussel and its capacity to alter the host immune response [11]. Herein, we expand the
259 knowledge on mussel-pathogen interactions by exploring infection dynamics via water tank
260 cohabitation experimental model and by studying hemocyte responses via *in vitro/in vivo*
261 assays.

262 **4.1. *In vitro* hemocyte-pathogen interactions**

263 To elicit cell-mediated immune responses, adhesion phenomena are crucial. In our experiments,
264 *V. splendidus* 10/068 1T1 severely altered hemocyte attachment to the culture substratum. After
265 2 hours of incubation in the presence of the virulent *Vibrio*, the number of non-adherent cells
266 was higher than in non-treated cultures or in cells co-incubated with the innocuous bacteria.
267 This effect increased after 6h of exposure to *V. splendidus* 10/068 1T1. Similar observations
268 were made for other *Vibrio* species with bivalve hemocytes. For example, *V. tasmaniensis*
269 LGP32 decreased hemocyte adhesion capacity in *Mytilus edulis* [29], *Mytilus galloprovincialis*
270 [30] and *Mya arenaria* [31]. The same response was reported for *Crassostrea gigas* hemocytes
271 challenged with *V. aestuarianus* 01/32 [32] and cells of *Ruditapes philippinarum* in contact
272 with *V. tapetis* [33]. Despite the robustness of these observations, specific mechanisms by
273 which a pathogen induces hemocyte detachment from adhesion surfaces remain poorly
274 understood. Some studies suggested the involvement of proteases secreted by the bacteria and
275 responsible for disruption of cytoskeleton, cell adhesion molecules and extracellular matrix
276 components. In the Pacific oyster, hemocyte treatment with extracellular products (ECPs) of *V.*
277 *aestuarianus* 01/32 or *V. tubiashii* 07/118 T2 inhibited cell binding to culture dish [34,35].
278 Furthermore, the hydrolytic action of extracellular effectors capable to degrade muscle
279 collagen, bovine actin and fibronectin proteins has been shown [35]. In addition of abolishing
280 hemocyte attachment to substrate, alteration of immunocyte adhesion capabilities by ECPs also

281 probably affects phagocyte activity. In this regard, we have previously shown that ECPs from
282 *V. splendidus* 10/068 1T1 inhibit *M. edulis* hemocyte phagocytosis [11].

283 Upon entrance into hemocytes, the fate of bacteria depends on phagosome biogenesis and
284 maturation. Intracellular trafficking and killing of engulfed microorganisms is a highly
285 choreographed process driven by subsequent fusion and fission events during which the
286 maturing phagosome acquires the characteristics of degradative acidic lysosomes [36,37]. In
287 our study, *V. splendidus* 10/068 1T1 inhibited acidic vacuole formation in mussel hemocytes
288 while the innocuous phylogenetically related to *V. splendidus* 12/056 M24T1 had no effect.
289 Such mechanism has been described for intracellular pathogens as strategy to survive and
290 maintain infection within cells. This is the case of *Legionella pneumophila*, the causative agent
291 of Legionnaire's pneumonia, known for its ability to manipulate host cell vesicular trafficking
292 pathways and to inhibit phagosome-lysosome fusion [38,39]. In the same way, *Mycobacterium*
293 sp. reside inside vacuoles and arrest the fusion with late endosomal/lysosomal organelles [40,
294 41]. For *Vibrio* species, few reports have shown their capacity to adopt intracellular stages [42–
295 44]. To our knowledge, only *V. tasmaniensis* LGP32 has been described as a facultative
296 intracellular pathogen of the Pacific oyster, able to modulate phagosome maturation as well as
297 oxidative response [24]. More recently, Vanhove et al. [45] showed the intracellular surviving
298 of this strain until hemocyte cytolysis (more than 25% of cell lysis after 17h incubation). In
299 accordance with these findings, it seems that *V. splendidus* 10/068 1T1 displays a similar
300 infection strategy to *V. tasmaniensis* LGP32. Besides altering phagosome maturation and ROS
301 production [11], this *Mytilus edulis* pathogen affected hemocyte viability and induced almost
302 39% of dead cells after 18h. The latter point prove the cytotoxicity of the bacteria and suggests
303 its surviving into the cells.

304 **4.2. *In vivo* infection dynamics**

305 Understanding pathogenesis processes requires an animal model of infection [46]. In our
306 previous study, we have demonstrated the virulence of *V. splendidus* 10/068 1T1 towards the
307 blue mussel by injection [11]. In spite its efficacy and repeatability, this method does not reflect
308 the realistic way of host-bacteria interaction. Herein, we successfully reproduced experimental
309 infection by cohabitation assays. In these experimental conditions, first mortalities appeared
310 after 3 days and increased progressively suggesting a necessity of time for bacteria transfer
311 from diseased animals and the occurrence of a latency period in healthy mussels. At the same
312 time intervals, the amount of GFP-*Vibrio* released in the seawater decreased ($3 \cdot 10^6$ CFU/mL at
313 the 2nd day to $2 \cdot 10^3$ CFU/mL at the 6th day). In addition to probable adhesion/penetration into

314 its host, this decline could result from bacteria mortality or adhesion to tank walls. Though,
315 *Vibrio* were also detected in healthy mussel tissues confirming a transmission of a part of them
316 from infected animals during the cohabitation period.

317 Up to now, only few works have investigated non-invasive methods for the study of infectious
318 diseases in bivalves and they were limited to Pacific oysters. In this model, successful
319 experimental vibriosis were induced by cohabitation [47,48] or by immersion assays [49]. In
320 our case, unlike cohabitation experiments, the bathing procedure did not cause any mortality
321 (data not shown). This negative result reveals the complexity of infection process. Bacteria may
322 require a priming infectious niche or a cooperation with mussel microflora to initiate some
323 virulence mechanisms [50].

324 During experimental infection, the number of circulating cells temporary increased at day 2
325 post-challenge and then stabilized to a value not distinct from control. Similar transient
326 hemocytosis have been described in diverse bivalve species like *M. edulis* [51], *M.*
327 *galloprovincialis* [52] and *R. philippinarum* [53] in response to physical stresses or pathogen
328 threats. Such variation in circulating hemocytes have been explained by cell proliferation [51].
329 Mobilizations of peripheral hemocytes from tissues consecutively to bacterial infection were
330 also evoked to account for by a transient increase of circulating cells [32,53]. Inversely, back
331 infiltration of infected sites by hemocytes could explain a consecutive decrease of total
332 hemocyte count in hemolymph. Alternatively, the decrease of cell concentration observed
333 secondarily to hemocytosis can also originate from a *Vibrio* induced hemocyte death. The
334 hypothesis get confirmation from our experiments showing a loss of viability both for
335 hemocytes exposed to *Vibrio in vitro* and for hemocytes withdraw from infected animals. It is
336 also in good agreement with mortalities observed after 3 days of cohabitation with septic
337 mussels. Furthermore, *V. splendidus* 10/068 1T1 was detected in hemocytes and the population
338 of bacteria-containing hemocyte declined progressively with time. The latter result is probably
339 coherent with a pathogenicity involving a phagocyte lysis and a bacteria release.

340 In addition to hemocyte parameters analysis, histology was performed on infected mussels.
341 Many organisms were identified in tissues of living and moribund mussel (trematodes,
342 copepods, *Ciliophora*, ciliates and gregarines). The presence of parasites is not surprising since
343 animals were collected from natural areas. Their potential interaction with pathogens are still
344 unknown. GFP-*Vibrio* were localized in diverse organs and obviously caused necrosis of
345 digestive gland and gills principally. Data concerning bacterial diseases in bivalves indicate that
346 infections are initiated at mucosal interfaces [54]. Nevertheless, in order to establish a

347 chronology, the entry route of bacteria has to be identified. Few studies explored portal access
348 of pathogens in bivalves. For example, the organic matrix of the shell has been described as a
349 putative entryway of the pathogenic *V. tapetis* in the clam *R. philippinarum* [55,56]. More
350 recently, a study suggested the involvement of hemocytes in microbe transport because of their
351 ability to migrate across mucosal epithelia and to translocate within hours from pallial surfaces
352 to underlying tissues and to the circulatory system [54]. This hypothesis may be plausible in
353 our study considering the cytotoxicity of *V. splendidus* 10/068 1T1 to hemocytes. Further
354 investigations at the first hours of infection are needed to elucidate whether hemocytes are the
355 first or the last target of pathogens.

356 **5. Conclusion**

357 *V. splendidus* 10/068 1T1 has been previously reported to be pathogenic to the blue mussel. In
358 this study, we first investigated hemocyte-bacteria interactions. *In vitro* challenges demonstrate
359 the capacity of *Vibrio* strain to alter the maturation of the phagolysosome, the cell adhesion and
360 viability. Then, we successfully established a non-invasive experimental infection model via
361 cohabitation. Bacteria were able to bypass defense barriers and were detected in diverse organs
362 and in hemocytes. The number and the viability of circulating hemocytes were altered. Taken
363 together, our results confirm the virulence of *V. splendidus* 10/068 1T1 towards *M. edulis*
364 hemocytes and suggest the use of immune cells as pathogen vehicles to spread the infection in
365 the whole organism. Furthermore, besides the description of an original infection process, this
366 study can be useful to be compared with natural mortalities occurred in the field.

367 **Acknowledgements**

368 This work received fundings from the State/Region Plan Contract (CPER) allocated through
369 the Research Federation FR CNRS 3730 SCALE /FED 4116 SCALE (Sciences Appliquées à
370 L'Environnement), and DGAI support through National Reference Laboratory activities for
371 mollusc diseases (Ifremer-La Tremblade). Yosra Ben Cheikh was a recipient for a Ph.D. grant
372 from the Conseil Regional de Haute-Normandie. The authors are indebted to the marine fish
373 farm Aquacaux (Octeville, France) and Histalim (Montpellier, France) for valuable technical
374 assistance.

375

376

377 **References**

- 378 [1] Thompson, F.L., Iida, T., Swings, J., **2004**. Biodiversity of *Vibrios*. *Microbiol. Mol. Biol.*
379 *Rev.* 68, 403–431. doi:10.1128/MMBR.68.3.403-431.2004
- 380 [2] Hasan, N.A., Grim, C.J., Lipp, E.K., Rivera, I.N.G., Chun, J., Haley, B.J., Taviani, E.,
381 Choi, S.Y., Hoq, M., Munk, A.C., Brettin, T.S., Bruce, D., Challacombe, J.F., Detter,
382 J.C., Han, C.S., Eisen, J.A., Huq, A., Colwell, R.R., **2015**. Deep-sea hydrothermal vent
383 bacteria related to human pathogenic *Vibrio* species. *Proc. Natl. Acad. Sci.* 112, E2813–
384 E2819. doi:10.1073/pnas.1503928112
- 385 [3] Travers, M.-A., Boettcher Miller, K., Roque, A., Friedman, C.S., **2015**. Bacterial
386 diseases in marine bivalves. *J. Invertebr. Pathol.* doi:10.1016/j.jip.2015.07.010
- 387 [4] Feldhusen, F., **2000**. The role of seafood in bacterial foodborne diseases. *Microbes*
388 *Infect.* 2, 1651–1660. doi:10.1016/S1286-4579(00)01321-6
- 389 [5] Powell, J.L., **1999**. *Vibrio* species. *Clin. Lab. Med.* 19, 537–552, vi.
- 390 [6] Colwell, R.R., Grimes, D.J., **1984**. *Vibrio* diseases of marine fish populations.
391 *Helgoländer Meeresunters.* 37, 265–287. doi:10.1007/BF01989311
- 392 [7] Ben-Haim, Y., Rosenberg, E., **2002**. A novel *Vibrio* sp. pathogen of the coral
393 *Pocillopora damicornis*. *Mar. Biol.* 141, 47–55. doi:10.1007/s00227-002-0797-6
- 394 [8] Goarant, C., Ansquer, D., Herlin, J., Domalain, D., Imbert, F., De Decker, S., **2006**.
395 “Summer Syndrome” in *Litopenaeus stylirostris* in New Caledonia: Pathology and
396 epidemiology of the etiological agent, *Vibrio nigripulchritudo*. *Aquaculture* 253, 105–
397 113. doi:10.1016/j.aquaculture.2005.07.031
- 398 [9] Paillard, C., Le Roux, F., Borrego, J.J., **2004**. Bacterial disease in marine bivalves, a
399 review of recent studies: Trends and evolution. *Aquat. Living Resour.* 17, 477–498.
400 doi:10.1051/alr:2004054
- 401 [10] Beaz-Hidalgo, R., Balboa, S., Romalde, J.L., Figueras, M.J., **2010a**. Diversity and
402 pathogenicity of *Vibrio* species in cultured bivalve molluscs. *Environ. Microbiol. Rep.*
403 2, 34–43. doi:10.1111/j.1758-2229.2010.00135.x
- 404 [11] Ben Cheikh, Y., Travers, M.-A., Morga, B., Godfrin, Y., Rioult, D., Le Foll, F., **2016**.
405 First evidence for a *Vibrio* strain pathogenic to *Mytilus edulis* altering hemocyte immune
406 capacities. *Dev. Comp. Immunol.* 57, 107–119. doi:10.1016/j.dci.2015.12.014
- 407 [12] Kwan, T.N., Bolch, C.J.S., **2015**. Genetic diversity of culturable *Vibrio* in an Australian
408 blue mussel *Mytilus galloprovincialis* hatchery. *Dis. Aquat. Organ.* 116, 37–46.
409 doi:10.3354/dao02905
- 410 [13] Bruto, M., James, A., Petton, B., Labreuche, Y., Chenivesse, S., Alunno-Bruscia, M.,
411 Polz, M.F., Le Roux, F., **2017**. *Vibrio crassostreae*, a benign oyster colonizer turned into
412 a pathogen after plasmid acquisition. *ISME J.* 11, 1043–1052.
413 doi:10.1038/ismej.2016.162
- 414 [14] Gay, M., Berthe, F.C.J., Le Roux, F., **2004**. Screening of *Vibrio* isolates to develop an
415 experimental infection model in the Pacific oyster *Crassostrea gigas*. *Dis. Aquat. Organ.*
416 59, 49–56. doi:10.3354/dao059049
- 417 [15] Lacoste, A., Jalabert, F., Malham, S., Cueff, A., Gélébart, F., Cordevant, C., Lange, M.,
418 Poulet, S.A., **2001**. A *Vibrio splendidus* strain is associated with summer mortality of
419 juvenile oysters *Crassostrea gigas* in the Bay of Morlaix (North Brittany, France). *Dis.*
420 *Aquat. Organ.* 46, 139–145. doi:10.3354/dao046139
- 421 [16] Lemire, A., Goudenège, D., Versigny, T., Petton, B., Calteau, A., Labreuche, Y., Le
422 Roux, F., **2015**. Populations, not clones, are the unit of *Vibrio* pathogenesis in naturally
423 infected oysters. *ISME J.* 9, 1523–1531. doi:10.1038/ismej.2014.233
- 424 [17] Saulnier, D., De Decker, S., Haffner, P., Cobret, L., Robert, M., Garcia, C., **2010**. A
425 large-scale epidemiological study to identify bacteria pathogenic to Pacific oyster
426 *Crassostrea gigas* and correlation between virulence and metalloprotease-like activity.
427 *Microb. Ecol.* 59, 787–798. doi:10.1007/s00248-009-9620-y

- 428 [18] Lambert, C., Nicolas, J.L., Cilia, V., **1999**. *Vibrio splendidus*-related strain isolated from
429 brown deposit in scallop (*Pecten maximus*) cultured in Brittany (France). *Bull Eur Fish*
430 *Pathol* 102.
- 431 [19] Nicolas, J.L., Corre, S., Gauthier, G., Robert, R., Ansquer, D., **1996**. Bacterial problems
432 associated with scallop *Pecten maximus* larval culture. *Dis. Aquat. Org.* 27, 67–76.
433 doi:10.3354/dao027067
- 434 [20] Beaz-Hidalgo, R., Diéguez, A.L., Cleenwerck, I., Balboa, S., Doce, A., de Vos, P.,
435 Romalde, J.L., **2010b**. *Vibrio celticus* sp. nov., a new *Vibrio* species belonging to the
436 *Splendidus* clade with pathogenic potential for clams. *Syst. Appl. Microbiol.* 33, 311–
437 315. doi:10.1016/j.syapm.2010.06.007
- 438 [21] Kesarcodi-Watson, A., Kaspar, H., Lategan, M.J., Gibson, L., **2009**. Two pathogens of
439 Greenshell mussel larvae, *Perna canaliculus*: *Vibrio splendidus* and a *V.*
440 *coralliilyticus/neptunius*-like isolate. *J. Fish Dis.* 32, 499–507. doi:10.1111/j.1365-
441 2761.2009.01006.x
- 442 [22] Araya, M.T., Siah, A., Mateo, D.R., Markham, F., McKenna, P., Johnson, G.R., Berthe,
443 F.C.J., **2009**. Morphological and molecular Effects of *Vibrio splendidus* on hemocytes of
444 softshell clams, *Mya arenaria*. *J. Shellfish Res.* 28, 751–758. doi:10.2983/035.028.0403
- 445 [23] Balbi, T., Fabbri, R., Cortese, K., Smerilli, A., Ciacci, C., Grande, C., Vezzulli, L.,
446 Pruzzo, C., Canesi, L., **2013**. Interactions between *Mytilus galloprovincialis* hemocytes
447 and the bivalve pathogens *Vibrio aestuarianus* 01/032 and *Vibrio splendidus* LGP32.
448 *Fish Shellfish Immunol.* 35, 1906–1915. doi:10.1016/j.fsi.2013.09.027
- 449 [24] Duperthuy, M., Schmitt, P., Garzón, E., Caro, A., Rosa, R.D., Le Roux, F., Lautrédou-
450 Audouy, N., Got, P., Romestand, B., de Lorgeril, J., Kieffer-Jaquinod, S., Bachère, E.,
451 Destoumieux-Garzón, D., **2011**. Use of OmpU porins for attachment and invasion of
452 *Crassostrea gigas* immune cells by the oyster pathogen *Vibrio splendidus*. *Proc. Natl.*
453 *Acad. Sci. U. S. A.* 108, 2993–2998. doi:10.1073/pnas.1015326108
- 454 [25] Restif, O., Graham, A.L., **2015**. Within-host dynamics of infection: from ecological
455 insights to evolutionary predictions. *Phil Trans R Soc B* 370, 20140304.
456 doi:10.1098/rstb.2014.0304
- 457 [26] Nyholm, S.V., Stabb, E.V., Ruby, E.G., McFall-Ngai, M.J., **2000**. Establishment of an
458 animal–bacterial association: Recruiting symbiotic *Vibrios* from the environment. *Proc.*
459 *Natl. Acad. Sci.* 97, 10231–10235. doi:10.1073/pnas.97.18.10231
- 460 [27] Nyholm, S.V., McFall-Ngai, M.J., **2003**. Dominance of *Vibrio fischeri* in secreted mucus
461 outside the light organ of *Euprymna scolopes*: the first site of symbiont specificity. *Appl.*
462 *Environ. Microbiol.* 69, 3932–3937.
- 463 [28] Cabello, A.E., Espejo, R.T., Romero, J., **2005**. Tracing *Vibrio parahaemolyticus* in
464 oysters (*Tiostrea chilensis*) using a Green Fluorescent Protein tag. *J. Exp. Mar. Biol.*
465 *Ecol.* 327, 157–166.
- 466 [29] Tanguy, M., McKenna, P., Gauthier-Clerc, S., Pellerin, J., Danger, J.-M., Siah, A., **2013**.
467 Functional and molecular responses in *Mytilus edulis* hemocytes exposed to bacteria,
468 *Vibrio splendidus*. *Dev. Comp. Immunol.* 39, 419–429. doi:10.1016/j.dci.2012.10.015
- 469 [30] Ciacci, C., Betti, M., Canonico, B., Citterio, B., Roch, P., Canesi, L., **2010**. Specificity of
470 anti-*Vibrio* immune response through p38 MAPK and PKC activation in the hemocytes
471 of the mussel *Mytilus galloprovincialis*. *J. Invertebr. Pathol.* 105, 49–55.
472 doi:10.1016/j.jip.2010.05.010
- 473 [31] Mateo, D.R., Siah, A., Araya, M.T., Berthe, F.C.J., Johnson, G.R., Greenwood, S.J.,
474 **2009**. Differential *in vivo* response of soft-shell clam hemocytes against two strains of
475 *Vibrio splendidus*: Changes in cell structure, numbers and adherence. *J. Invertebr.*
476 *Pathol.* 102, 50–56. doi:10.1016/j.jip.2009.06.008

- 477 [32] Labreuche, Y., Lambert, C., Soudant, P., Boulo, V., Huvet, A., Nicolas, J.-L., **2006a**.
478 Cellular and molecular hemocyte responses of the Pacific oyster, *Crassostrea gigas*,
479 following bacterial infection with *Vibrio aestuarianus* strain 01/32. *Microbes Infect.* 8,
480 2715–2724. doi:10.1016/j.micinf.2006.07.020
- 481 [33] Choquet, G., Soudant, P., Lambert, C., Nicolas, J.-L., Paillard, C., **2003**. Reduction of
482 adhesion properties of *Ruditapes philippinarum* hemocytes exposed to *Vibrio tapetis*.
483 *Dis. Aquat. Organ.* 57, 109–116. doi:10.3354/dao057109
- 484 [34] Labreuche, Y., Soudant, P., Gonçalves, M., Lambert, C., Nicolas, J.-L., **2006b**. Effects
485 of extracellular products from the pathogenic *Vibrio aestuarianus* strain 01/32 on
486 lethality and cellular immune responses of the oyster *Crassostrea gigas*. *Dev. Comp.*
487 *Immunol.* 30, 367–379. doi:10.1016/j.dci.2005.05.003
- 488 [35] Mersni-Achour, R., Imbert-Auvray, N., Huet, V., Ben Cheikh, Y., Faury, N., Doghri, I.,
489 Rouatbi, S., Bordenave, S., Travers, M.-A., Saulnier, D., Fruitier-Arnaudin, I., **2014**.
490 First description of French *V. tubiashii* strains pathogenic to mollusk: II.
491 Characterization of properties of the proteolytic fraction of extracellular products. *J.*
492 *Invertebr. Pathol.* 123, 49–59. doi:10.1016/j.jip.2014.09.006
- 493 [36] Russell, D.G., 2001. Phagocytosis, in: ELS. John Wiley & Sons, Ltd.
- 494 [37] Weiss, G., Schaible, U.E., **2015**. Macrophage defense mechanisms against intracellular
495 bacteria. *Immunol. Rev.* 264, 182–203. doi:10.1111/imr.12266
- 496 [38] Horwitz, M.A., **1983**. The Legionnaires' disease bacterium (*Legionella pneumophila*)
497 inhibits phagosome-lysosome fusion in human monocytes. *J. Exp. Med.* 158, 2108–
498 2126.
- 499 [39] Isberg, R.R., O'Connor, T., Heidtman, M., **2009**. The *Legionella pneumophila*
500 replication vacuole: making a cozy niche inside host cells. *Nat. Rev. Microbiol.* 7, 13–
501 24. doi:10.1038/nrmicro1967
- 502 [40] Armstrong, J.A., Hart, P.D., **1971**. Response of cultured macrophages to *Mycobacterium*
503 *tuberculosis*, with observations on fusion of lysosomes with phagosomes. *J. Exp. Med.*
504 134, 713–740.
- 505 [41] Russell, D.G., Mwandumba, H.C., Rhoades, E.E., **2002**. *Mycobacterium* and the coat of
506 many lipids. *J. Cell Biol.* 158, 421–426. doi:10.1083/jcb.200205034
- 507 [42] Rosenberg, E., Falkovitz, L., **2004**. The *Vibrio shiloi/Oculina patagonica* model system
508 of coral bleaching. *Annu. Rev. Microbiol.* 58, 143–159.
509 doi:10.1146/annurev.micro.58.030603.123610
- 510 [43] Santos, M. de S., Orth, K., **2014**. Intracellular *Vibrio parahaemolyticus* escapes the
511 vacuole and establishes a replicative niche in the cytosol of epithelial cells. *mBio* 5,
512 e01506-14. doi:10.1128/mBio.01506-14
- 513 [44] Zhang, L., Krachler, A.M., Broberg, C.A., Li, Y., Mirzaei, H., Gilpin, C.J., Orth, K.,
514 **2012**. Type III effector VopC mediates invasion for *Vibrio* species. *Cell Rep.* 1, 453–
515 460. doi:10.1016/j.celrep.2012.04.004
- 516 [45] Vanhove, A.S., Rubio, T.P., Nguyen, A.N., Lemire, A., Roche, D., Nicod, J., Vergnes,
517 A., Poirier, A.C., Disconzi, E., Bachère, E., Le Roux, F., Jacq, A., Charrière, G.M.,
518 Destoumieux-Garzón, D., **2016**. Copper homeostasis at the host *Vibrio* interface: lessons
519 from intracellular *Vibrio* transcriptomics. *Environ. Microbiol.* 18, 875–888.
520 doi:10.1111/1462-2920.13083
- 521 [46] Le Roux, F.L., Wegner, K.M., Polz, M.F., **2016**. Oysters and **Vibrios** as a Model for
522 Disease Dynamics in Wild Animals. *Trends Microbiol.* 24, 568–580.
523 doi:10.1016/j.tim.2016.03.006
- 524 [47] Azéma, P., Travers, M.-A., De Lorgeril, J., Tourbiez, D., Dégremont, L., **2015**. Can
525 selection for resistance to OsHV-1 infection modify susceptibility to *Vibrio aestuarianus*

- 526 infection in *Crassostrea gigas*? First insights from experimental challenges using
527 primary and successive exposures. *Vet. Res.* 46. doi:10.1186/s13567-015-0282-0
- 528 [48] De Decker, S., Saulnier, D., **2011**. Vibriosis induced by experimental cohabitation in
529 *Crassostrea gigas*: Evidence of early infection and down-expression of immune-related
530 genes. *Fish Shellfish Immunol.* 30, 691–699. doi:10.1016/j.fsi.2010.12.017
- 531 [49] De Decker, S., Normand, J., Saulnier, D., Pernet, F., Castagnet, S., Boudry, P., **2011**.
532 Responses of diploid and triploid Pacific oysters *Crassostrea gigas* to *Vibrio* infection in
533 relation to their reproductive status. *J. Invertebr. Pathol.* 106, 179–191.
534 doi:10.1016/j.jip.2010.09.003
- 535 [50] Harrison, F., 2013. Bacterial cooperation in the wild and in the clinic: Are pathogen
536 social behaviours relevant outside the laboratory? *Bioessays* 35, 108–112.
537 doi:10.1002/bies.201200154
- 538 [51] Renwrantz, L., Siegmund, E., Woldmann, M., **2013**. Variations in hemocyte counts in
539 the mussel, *Mytilus edulis*: similar reaction patterns occur in disappearance and return of
540 molluscan hemocytes and vertebrate leukocytes. *Comp. Biochem. Physiol. A. Mol.*
541 *Integr. Physiol.* 164, 629–637. doi:10.1016/j.cbpa.2013.01.021
- 542 [52] Ciacci, C., Citterio, B., Betti, M., Canonico, B., Roch, P., Canesi, L., **2009**. Functional
543 differential immune responses of *Mytilus galloprovincialis* to bacterial challenge. *Comp.*
544 *Biochem. Physiol. B Biochem. Mol. Biol.* 153, 365–371. doi:10.1016/j.cbpb.2009.04.007
- 545 [53] Allam, B., Paillard, C., Auffret, M., Ford, S.E., **2006**. Effects of the pathogenic *Vibrio*
546 *tapetis* on defence factors of susceptible and non-susceptible bivalve species: II. Cellular
547 and biochemical changes following *in vivo* challenge. *Fish Shellfish Immunol.* 20, 384–
548 397. doi:10.1016/j.fsi.2005.05.013
- 549 [54] Allam, B., Pales Espinosa, E., **2016**. Bivalve immunity and response to infections: Are
550 we looking at the right place? *Fish Shellfish Immunol.*, Special Issue: ISFSI 2016 53, 4–
551 12. doi:10.1016/j.fsi.2016.03.037
- 552 [55] Allam, B., Paillard, C., Ford, S.E., **2002**. Pathogenicity of *Vibrio tapetis*, the etiological
553 agent of brown ring disease in clams. *Dis. Aquat. Organ.* 48, 221–231.
554 doi:10.3354/dao048221
- 555 [56] Paillard, C., Maes, P., **1995**. The Brown Ring Disease in the Manila Clam, *Ruditapes*
556 *philippinarum*. *J. Invertebr. Pathol.* 65, 91–100. doi:10.1006/jipa.1995.1015
- 557
- 558
- 559
- 560
- 561
- 562
- 563
- 564
- 565
- 566

567 **Figure legend**

568 **Figure 1.** Effect of *V. splendidus*-related strains on hemocyte adhesion *in vitro*.
569 The number of non-adherent cells was evaluated after exposure to the virulent *V. splendidus*
570 10/068 1T1 and to the non-virulent *V. splendidus* 12/056 M24T1 for 2, 4 and 6h. Data are
571 expressed as mean \pm SEM (n=5), * indicates values significantly different from control and §
572 marks results that significantly differ from values obtained with the non-virulent bacteria
573 12/056 M24T1 (p<0.05, Student's t-test)

574 **Figure 2.** Acidic vacuole formation in hemocytes after exposure to *V. splendidus*-related
575 strains. (a) Flow cytometry analysis of hemocytes exposed *in vitro* to virulent or non-virulent
576 bacteria during 2h and incubated 30 min with lysotracker at 0.4 μ M. Data are expressed as mean
577 of fluorescence \pm SEM, arbitrary units (A.U.), n=5. *** indicates values significantly different
578 from control (Student's t-test, p<0.001). (b) Fluorescence microscopy of hemocytes exposed *in*
579 *vitro* to virulent or non-virulent bacteria during 2h and incubated with lysotracker green (0.4
580 μ M, 30 min) and Hoechst 33342 (5 μ M, 15 min).

581 **Figure 3.** Effect of exposure to bacteria on hemocyte viability *in vitro*. Hemocytes were
582 incubated with *V. splendidus*-related strains 10/068 1T1 or 12/056 M24T1 for different time
583 durations. Viability was determined by flow cytometry after propidium iodide staining. Data
584 are expressed as mean \pm SEM, n=4. ** indicates values significantly different from the control
585 p<0.01 Student's t-test).

586 **Figure 4.** Cumulative mortalities recorded after experimental infections of adult mussels by
587 water tank cohabitation with septic mussels. GFP-tagged *V. splendidus* 10/068 1T1 strain was
588 injected intramuscularly to mussels. 24h post injection, moribund animals were sacrificed and
589 placed in cohabitation with healthy mussels for 72h and then removed. Cohabitation assays
590 with mussels injected with FSSW were used as control. Data are mean \pm SEM of cumulative
591 mortalities in triplicate tanks.

592 **Figure 5.** *V. splendidus* 10/068 1T1 count in water tank seawater during experimental infections
593 *in vivo* by cohabitation with septic mussels. Seawater was sampled daily during cohabitation
594 assays and plated on LBS kanamycin agar plates. Bacteria concentration was determined over
595 time (CFU/mL, mean \pm SEM, n=3)

596 **Figure 6.** Analysis of hemocyte parameters during experimental infections by *V. splendidus*
597 10/068 1T1 via water tank cohabitation with septic mussels. Hemolymph was sampled over

598 time from cohabited mussels and (a) absolute hemocyte concentration, (b) percentage of
599 hemocyte containing GFP bacteria and (c) hemocyte viability were monitored by flow
600 cytometry. Data are expressed as mean \pm SEM (n=4-13). Values significantly different from
601 control are indicated (* p<0.05, ** p<0.01*, ***p<0.001, Student's t-test).

602 **Figure 7.** Histological observations of mussel tissues during experimental infections by *V.*
603 *splendidus* 10/068 1T1 via water tank cohabitation with septic mussels. GFP-tagged bacteria
604 were detected by immunohistochemistry (pink labeling). Tissues were counter-stained with
605 hematoxylin. A-C: Gills, D: esophagi and stomach. Scale bars of 50 or 100 μ m are indicated.

606 **Supplementary figure 1.** Histological observations of hematoxylin-eosin stained sections of
607 mussel tissues during experimental infections by water tank cohabitation with septic mussels.
608 A. Unidentified trematode in digestive glands (metacercaria), B. *Mytilicola* sp. in digestive lumen,
609 C. Unidentified copepod and hemocytes infiltration in gills, D. Bacteria, ciliates and gill
610 necrosis, E. Digestive glands and esophagi necrosis, F. Inflammatory granulomas. Scale bars
611 of 100 μ m, 250 μ m, 500 μ m or 1 mm are indicated.

612

613

614

615

616

617

618 **Table 1:** Histological observations on hematoxylin-eosin stained sections of mussel tissues
619 during experimental infections by water tank cohabitation with septic mussels. Presence of
620 micro-organisms and lesions (as necrosis, infiltrations or granulomas) were noticed and
621 classified in categories (0, 1, 2 or 3) as defined in material and methods section. A total of 40
622 individuals were observed (21 males, 19 females; 38 live sacrificed animals, 9 moribunds).
623 Number of observations is indicated, as well as the number of included moribunds in this
624 count (includ. xM = including x moribunds).

625

626

Figure 1

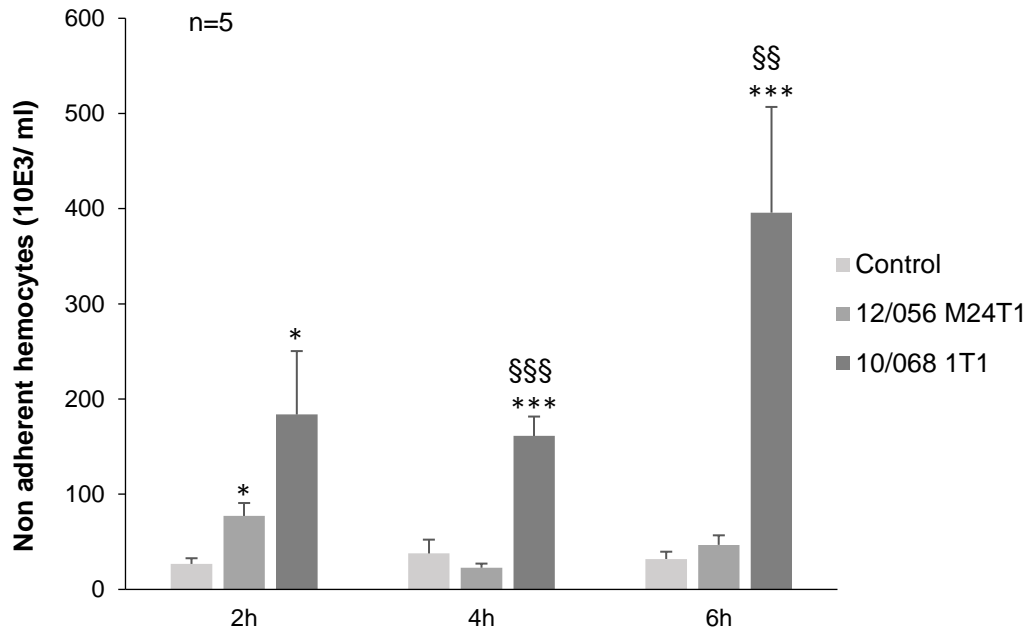
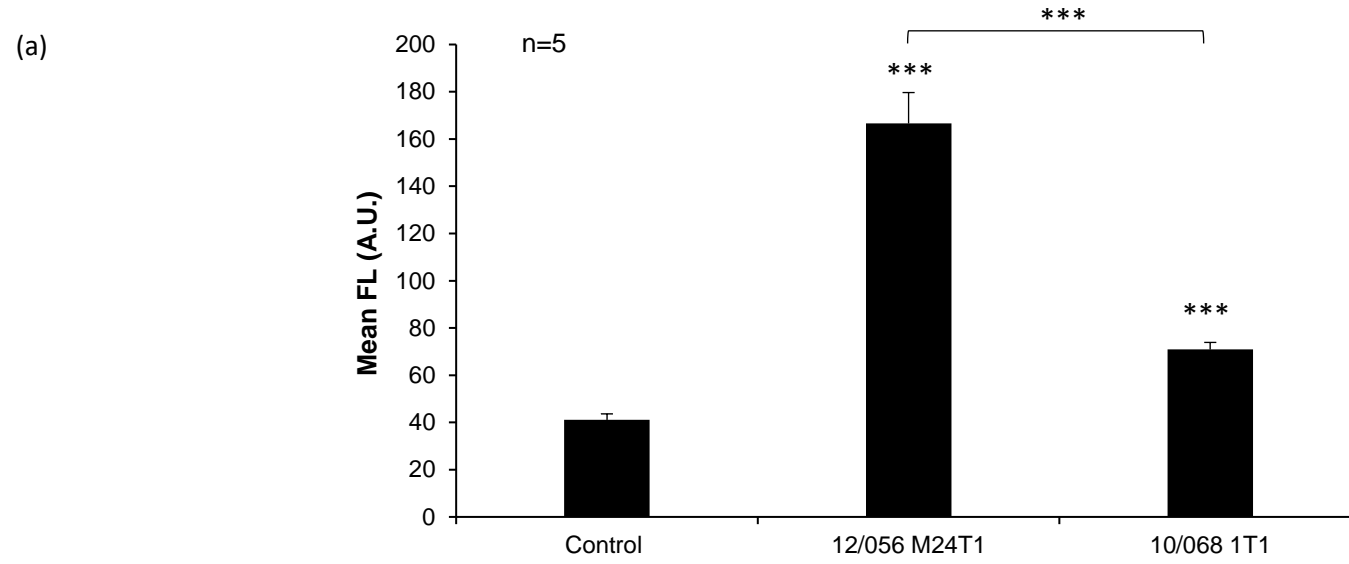


Figure 2



(b)

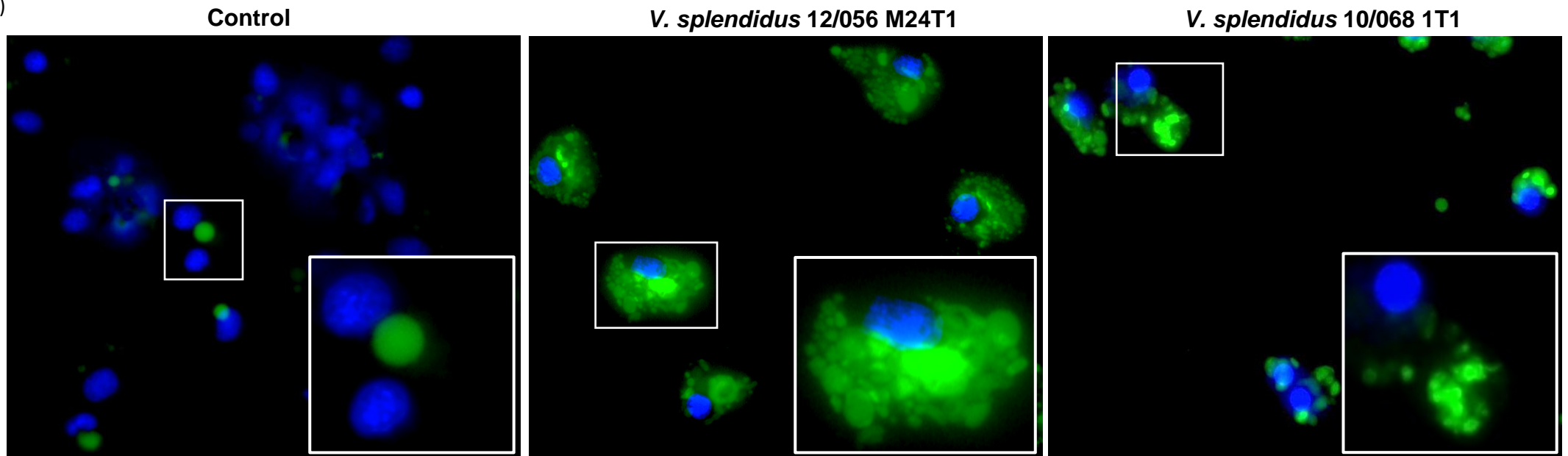


Figure 3

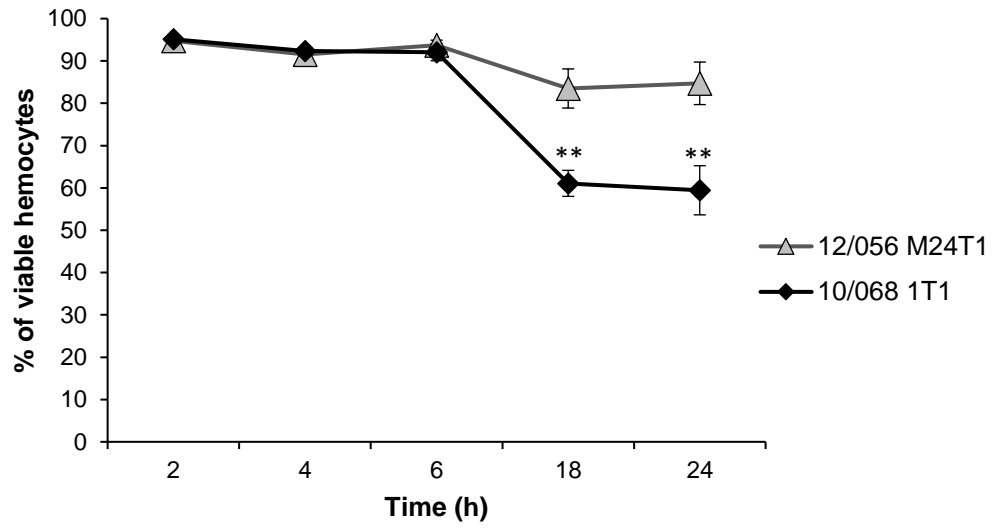


Figure 4

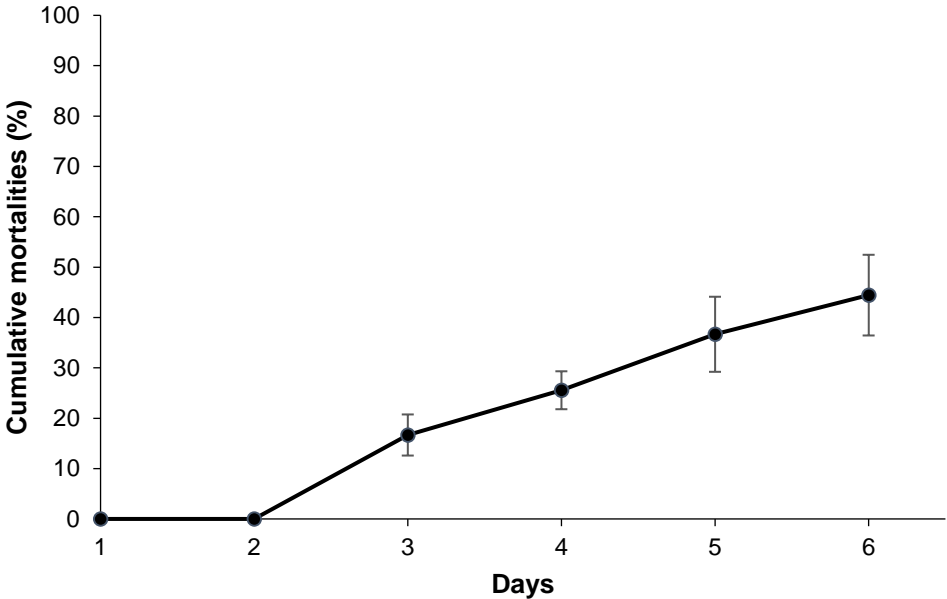


Figure 5

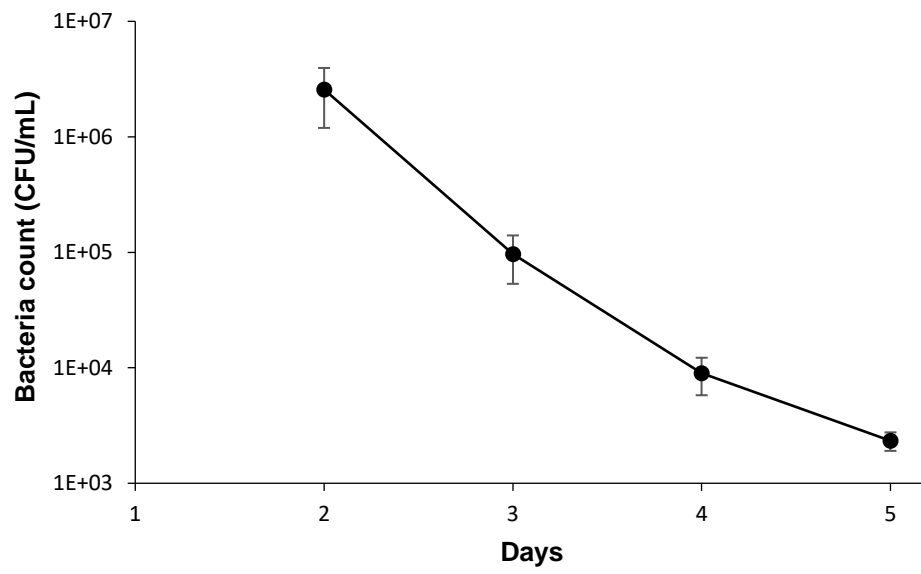
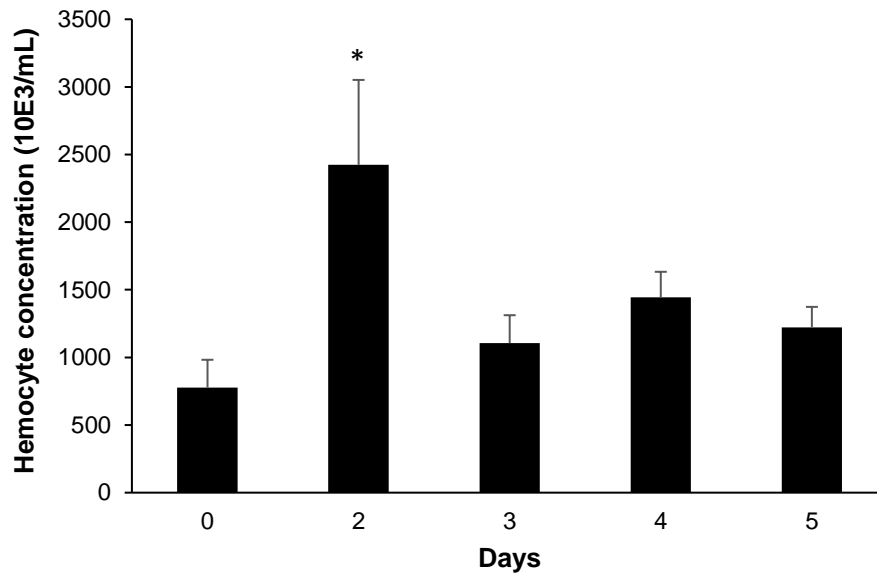
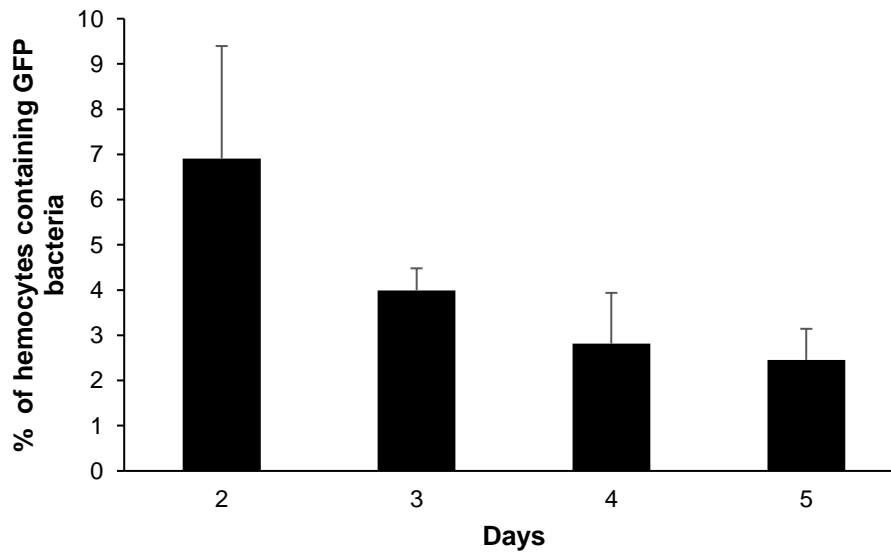


Figure 6

(a)



(b)



(c)

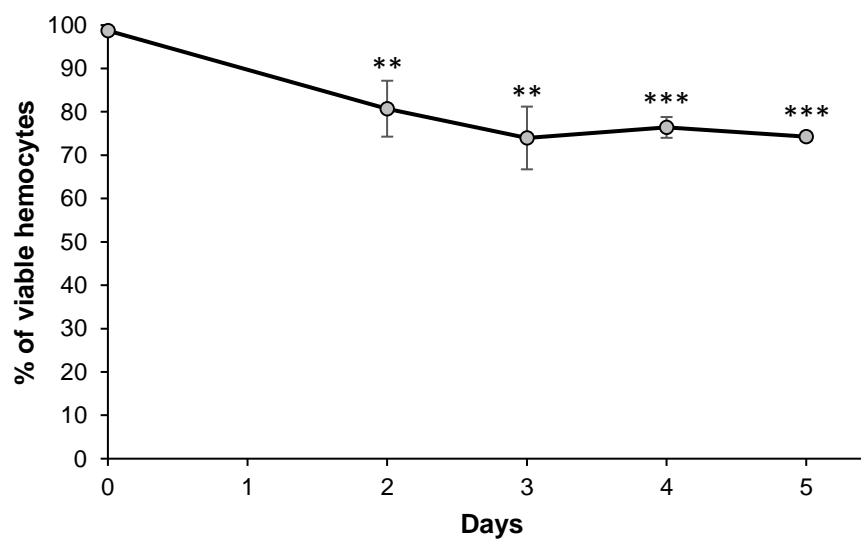
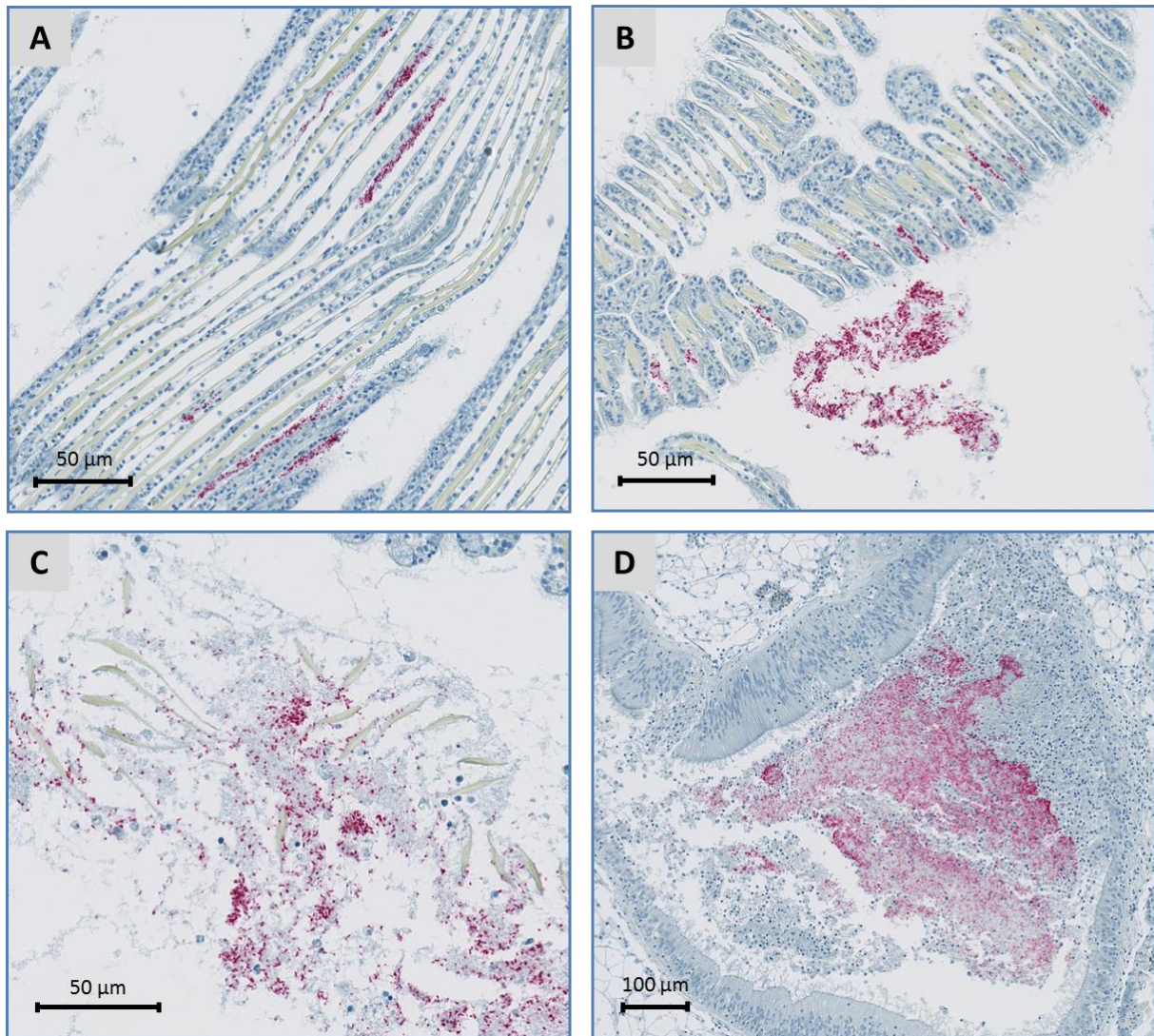


Figure 7



Supplementary figure 1

